

Degradation of a Wholly Aromatic Main-Chain Thermotropic Liquid-Crystalline Polymer Mediated by Superbases

Yuya Watanabe, Kazuki Fukushima,* and Takashi Kato*



Cite This: *JACS Au* 2024, 4, 2944–2956



Read Online

ACCESS |

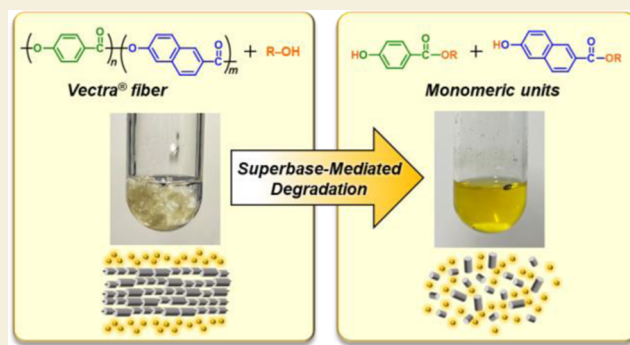
Metrics & More

Article Recommendations

Supporting Information

ABSTRACT: Plastic circular economy needs to be established to solve environmental issues related to plastic waste. Superengineering plastics such as liquid-crystalline (LC) polymers exhibit excellent thermal and mechanical properties, resulting in poor degradability in natural environment. Herein, we report the degradation of a wholly aromatic thermotropic LC polyester, poly(4-hydroxybenzoic acid-co-6-hydroxy-2-naphthoic acid) (Vectra) mediated by superbases. Methanolysis and hydrolysis of Vectra yield its monomeric compounds, 4-hydroxybenzoic acid, 6-hydroxy-2-naphthoic acid, and their methyl esters. Among several transesterification catalysts explored, 1,5,7-triazabicyclo[4.4.0]dec-5-ene (TBD) is the most suitable for the methanolysis of Vectra. The complete degradation of Vectra is achieved under reflux. The degradation proceeds heterogeneously via a surface erosion mechanism, preferentially starting from less chain-packed regions. Model reactions using aryl arylates reveal that monomeric compound–superbase complexes could mediate the cleavage of the ester bonds in both homogeneous and heterogeneous systems. The ester bonds of Vectra have inherent poor reactivity and are protected by oriented robust structures of the polymer. Nevertheless, the superbases enable the degradation of Vectra via the cleavage of the ester bonds by methanol. These outcomes open the way for recycling high-performance plastics as well as demonstrate the feasibility of recovering precious aromatic compounds from plastic waste as aromatic feedstock.

KEYWORDS: degradation, liquid-crystalline polymers, superbases, organocatalysts, chemical recycling



1. INTRODUCTION

Aromatic condensation polymers are widely used in our daily lives from packaging to structural materials due to their lightweight, low production cost, and mechanical and thermal stabilities. Liquid-crystalline (LC) polymeric materials have been gaining much attention as high-performance and functional materials.^{1–4} Main-chain thermotropic LC polymers such as Vectra, Econol, and X7G are aromatic polyesters that exhibit excellent mechanical and thermal properties by self-assembly and alignment of the rigid aromatic structures (Figure 1),^{5–9} and are known as superengineering plastics. Their outstanding physical properties include high moduli, low coefficients of thermal expansion, wide-range heat resistance, and ultraviolet (UV) resistance. Therefore, these LC polymers have been employed in fiber-reinforced composites, industrial ropes and cables, smartphone and automobile parts, aerospace materials, and sterilizable surgical instruments (Figure 1).^{10,11} Moreover, these LC polyesters are expected to contribute to the fifth-generation (5G) mobile network technology with 20 Gbps in printed circuit boards due to their low permittivity and moisture adsorption.¹² The relationships between chemical structures and properties of these aromatic polyesters have been extensively studied.^{13–19}

With the rising concerns and demands for environmental problems, the degradation and recycling of polymeric materials are of interest.²⁰ Conventional aromatic condensation polymers such as poly(ethylene terephthalate) (PET) and bisphenol A polycarbonate (BPA-PC) have been studied as the primary targets for plastic recycling.^{21,22} However, wholly aromatic polyesters are physically more stable than PET and BPA-PC; thus, their degradation and recycling are more challenging.

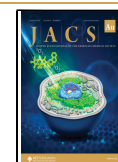
Some aliphatic polyesters and polycarbonates show biodegradability.^{23–25} These aliphatic condensation polymers have been considered as possible alternatives to petroleum-based and nondegradable polymers. As ester and carbonate bonds are cleaved by nucleophiles such as alcohols, amines, and water, the aliphatic condensation polymers are readily degraded in natural environment and in the human body with

Received: March 30, 2024

Revised: June 30, 2024

Accepted: July 2, 2024

Published: July 16, 2024



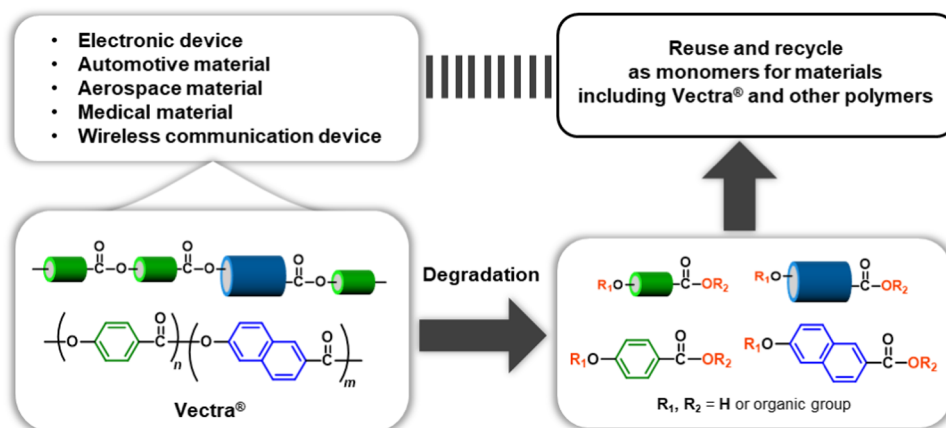


Figure 1. Schematic illustration of a strategy of the present study on wholly aromatic thermotropic polyesters.

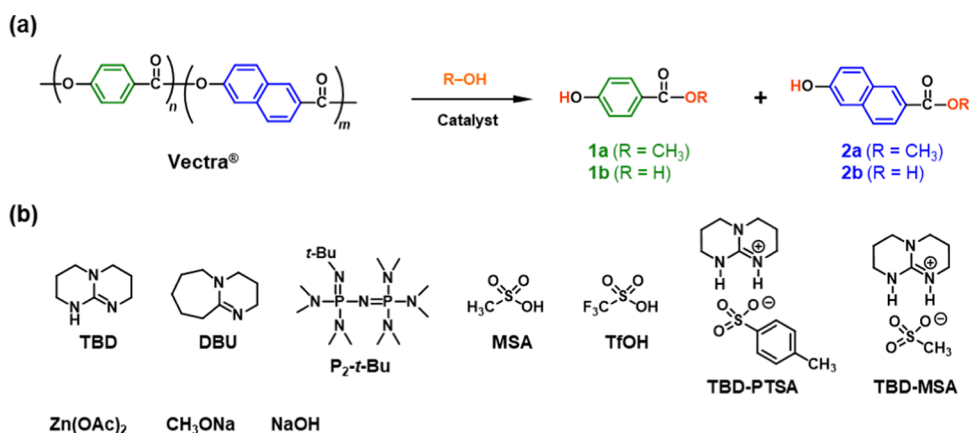


Figure 2. Degradation of Vectra using R–OH mediated by organic bases, acids, and salts. (a) Reaction scheme. (b) Catalysts tested in this study. TBD: 1,5,7-triazabicyclo[4.4.0]dec-5-ene; DBU: 1,8-diazabicyclo[5.4.0]undec-7-ene; P₂-*t*-Bu: 1-*tert*-butyl-2,2,4,4,4-pentakis-(dimethylamino)-2Λ⁵,4Λ⁵-catenadi(phosphazene); MSA: methanesulfonic acid; TfOH: trifluoromethanesulfonic acid; TBD-PTSA: 3,4,6,7,8,9-hexahydro-2*H*-pyrimido[1,2-*a*]pyrimidin-1-ium *p*-toluenesulfonate;⁷² TBD-MSA: 3,4,6,7,8,9-hexahydro-2*H*-pyrimido[1,2-*a*]pyrimidin-1-ium methanesulfonate.⁷³

the assistance of enzymes and microorganisms in some cases. The conventional aromatic condensation polymers are chemically and thermally stable, compared with aliphatic counterparts, and thus are difficult to degrade in natural environment. Accordingly, catalytic degradation of these aromatic condensation polymers using water, alcohols, and amines has been studied. As these degradation reactions proceed via transesterification, several transesterification catalysts have been examined, including conventional acids and bases,²⁶ organometallic complexes,^{27–29} and organic acids and bases.^{30–35} The catalytic degradation of PET and BPA-PC has been substantially investigated, leading to recent progress in efficient degradation and upcycling techniques.^{34–39} The scope of chemical recycling based on catalysis expands to polyolefins.^{40,41}

Utilizing biomass-based building blocks to construct polymeric materials is one approach to mitigate environmental impacts. However, for LC polyesters, it is not straightforward to develop biobased alternatives because of the difficulty in fulfilling such physical properties as high mechanical strength and wide-range heat resistance by biomass-based building blocks, although poly(ethylene furanoate) and poly(isosorbide carbonate) have been proposed as biomass-based alternatives to PET and BPA-PC, due to their comparable physical properties.^{42,43} Recent progress in biorelated technologies is

enabling biosynthesis and biomass-derived production of single aromatic compounds used in LC polyesters such as 4-hydroxybenzoic acid and hydroquinone.^{44–47} Nonetheless, highly valued fused aromatics and biphenyl derivatives used in the LC polyesters, such as 6-hydroxy-2-naphthoic acid and 4,4-biphenol, still rely on petroleum-based production.

Thermal reprocessing is a common recycling method employed for postconsumer thermoplastics, such as PET.²² However, LC polyesters exhibit a melting point of around 300 °C^{1,5–9} and their reprocessing at high temperature may lead to thermal degradation.⁴⁸ Furthermore, this condition is unpreferred from the aspect of energy consumption. Therefore, chemical recycling is a desirable option for the sustainable production of these LC polyesters (Figure 1).

Superengineering plastics, including LC polyesters, exhibit extremely high chemical stability in addition to outstanding mechanical and thermal properties. As results of these properties, they have become indispensable materials in various industrial fields. On the other hand, the inherent chemical inertness of these plastics hinders their chemical recyclability. Some degradation methods of these high-performance plastics have been reported.^{49–52} However, heating at high temperatures, excess additives and reagents, and high boiling-point solvents have been used to cleave bonds in such high-performance plastics. The efficient degradation of

high-performance plastics under relatively mild conditions was reported recently.⁵³ Exploring appropriate processing, dissolution, and catalysis should be a breakthrough for the chemical recycling and degradation of LC polyesters.

As is often reported for the solvolytic degradation of PET and BPA-PC, the reactions of these high-performance plastics proceed heterogeneously at the interface between the insoluble polymer and solvent. The efficiency of the reactions depends on the surface area of the substances. Homogeneous catalysts and solvents to swell the substances have been preferred for the heterogeneous degradation of PET and BPA-PC with low energy consumption to suppress the emission of greenhouse gases.^{54–56} Organocatalysts have been studied for the degradation of PET and BPA-PC since the 2010s. Among them, 1,5,7-triazabicyclo[4.4.0]dec-5-ene (TBD) and its derivatives are recognized as useful and potent catalysts.^{31,33} Recently, we reported that TBD-catalyzed methanolysis was the most suitable for the degradation of aliphatic polycarbonates, proceeding under ambient conditions.⁵⁷ We found that mesogenic triad aromatic esters were also degraded by the TBD-catalyzed methanolysis.⁵⁸ This result motivated us to investigate the efficacy of the organocatalysts, including TBD, in solvolytic degradation of wholly aromatic polyesters, which has never been examined.

Herein, we report on the successful degradation of Vectra, a main-chain thermotropic LC polyester consisting of 4-hydroxybenzoic acid and 6-hydroxy-2-naphthoic acid (Figure 2a). Methanolysis and hydrolysis are employed as means of the degradation of Vectra to care for the impact of degradation media on the environment. Methanol can be recognized as a green solvent in the future due to the production from biomass and CO₂ recently developed.^{59,60} Besides TBD, other superbases, sulfonic acids, and TBD-based salts are examined to find suitable degradation conditions (Figure 2b). This study will contribute to expanding the scope of polymer recycling to poorly degradable superengineering plastics, and furthermore, upgrading the LC polyesters as potentially recyclable SG materials.

2. RESULTS AND DISCUSSION

2.1. Methanolysis

The fiber form of a wholly aromatic polyester (Vectra) with a diameter of 23 μm (GoodFellow, Cambridge, U.K.) was cut into fragments with lengths of approximately 3 mm (Figure 3). Alcoholysis is often used in the catalytic degradation of condensation polymers, such as PET and BPA-PC, and proceeds heterogeneously. Methanolysis of Vectra was first conducted at 25 $^{\circ}\text{C}$, using organic bases and acids (Figure 2b). CH₃ONa⁶¹ was used as the reference. Generally, methanol was used in far excess of the ester bonds of Vectra (1.8 mL for 50 mg). Catalyst loading was fixed at 0.3 equiv relative to ester bonds in Vectra.

The degradation of Vectra proceeded under heterogeneous conditions as with those of other condensation polymers (Figure 3). No catalyst completed the methanolysis of Vectra under this condition, as the fibers were visually confirmed to remain in methanol even after 500 h. However, the supernatant became yellow, indicating the formation of methanol-soluble compounds. The supernatant was characterized by ¹H NMR spectroscopy. The spectra showed signals corresponding to the methyl esters of 4-hydroxybenzoic acid (1a) and 6-hydroxy-2-naphthoic acid (2a), along with those of

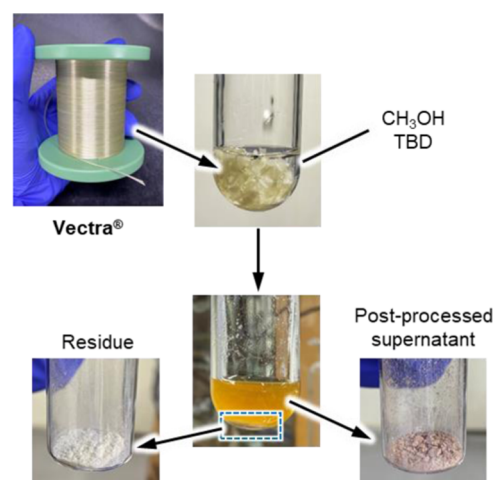


Figure 3. Typical methanolysis of Vectra using TBD, providing postprocessed supernatant and residue.

the catalysts used (Figure 4). The composition of 1a and 2a in the degradates was approximately 7:3, which was almost identical to the comonomer ratio in Vectra (73:27). The methanolysis using methanesulfonic acid (MSA),⁶² trifluoromethanesulfonic acid (TfOH),⁶² and CH₃ONa formed few soluble degradates at 25 $^{\circ}\text{C}$. In contrast, the organic bases, TBD, 1,8-diazabicyclo[5.4.0]-7-undecene (DBU),^{32,63,64} and 1-*tert*-butyl-2,2,4,4-pentakis-(dimethylamino)-2 Λ ⁵,4 Λ ⁵-catenadi(phosphazene) (P₂-*t*-Bu),^{65,66} facilitated methanolysis to some extent. These compounds have been shown to be effective in transesterification, including the degradation of polyesters and polycarbonates and ring-opening polymerization of cyclic esters and carbonates.^{67,68}

The progress of degradation was monitored based on the concentration of 1a and 2a dissolved in the supernatant calculated from the integral ratios of the degradates and catalysts (Figures 4 and S1), which were traced at several time points. Not surprisingly, TBD showed the highest activity to yield 28% of the monomeric esters from Vectra at 500 h, whereas DBU, P₂-*t*-Bu, and CH₃ONa slightly drove the reaction with the yields of 9, 7, and 2%, respectively (Figure 5a and Table S1). The specific activity of TBD, contrary to the expectation from its basicity (pK_a in acetonitrile = 26,⁶⁹ 24,⁷⁰ and 33⁷⁰ for TBD, DBU, and P₂-*t*-Bu, respectively), could be explained by the dual hydrogen-bonding activation mechanism, where sp² nitrogen and N–H activated alcohol (OH) and ester carbonyl (C=O) as hydrogen-bond acceptor and donor, respectively (Figure S2a).^{31,71} On the other hand, the other bases employed activate alcohol by serving as a hydrogen-bond acceptor or subtracting the hydrogen of the alcohol.^{63,65,68} The time analysis of the yields showed that TBD-facilitated methanolysis of Vectra reached a plateau at approximately 30% over 400 h (Figure 5a). The final yield (28%) was almost equal to the loading amount of TBD relative to the ester group of Vectra, implying the deactivation and consumption of the catalyst by the cleavage of the aryl ester.

The size-exclusion chromatography (SEC) profiles of the supernatants in the methanolysis using TBD, DBU, and CH₃ONa showed a predominant peak at 12 min and a small peak at approximately 11 min (Figure S3). These peaks could be attributed to the methyl esters of monomers 1a and 2a (Figure 2a) and their dimers. The degradation using P₂-*t*-Bu showed small multiple peaks at 10–11.5 min with the major

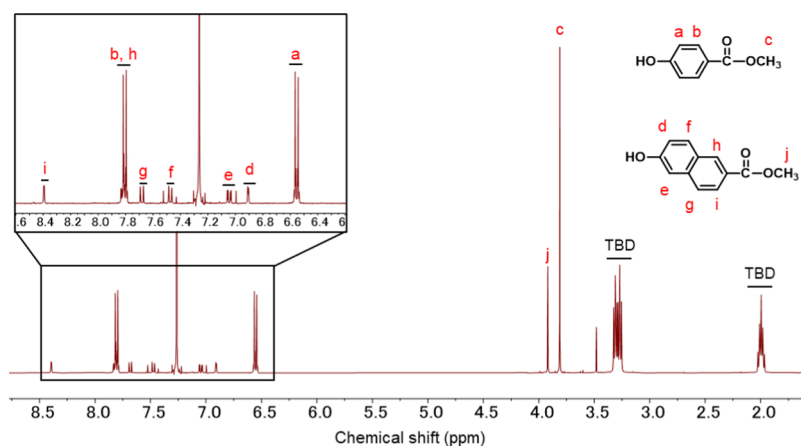


Figure 4. ^1H NMR spectrum (400 MHz in CDCl_3) of the supernatant in the methanolysis of Vectra using TBD (0.3 equiv) at 25 °C for 500 h.

monomer peak at 12 min, suggesting the formation of oligomers (Figure S3). The results of ^1H NMR and SEC studies of the methanolysis of Vectra at 25 °C suggests the potential of TBD to recover the monomeric esters from wholly aromatic polyesters efficiently.

TBD-based salts, 3,4,6,7,8,9-hexahydro-2*H*-pyrimido[1,2-*a*]-pyrimidin-1-ium *p*-toluenesulfonate (TBD-PTSA)⁷² and 3,4,6,7,8,9-hexahydro-2*H*-pyrimido[1,2-*a*]pyrimidin-1-ium methanesulfonate (TBD-MSA),⁷³ and zinc acetate were then employed as catalysts, along with MSA and TfOH in the methanolysis of Vectra under reflux conditions to enhance the effect of the reaction temperature. These salts are thermally stable and facilitate transesterification under heating conditions. However, no degradation was observed (Table S2, entries 6–12). This might be due to the low reaction temperature applied in the present study since these salts are used as a catalyst at above 180 °C, and their catalytic activities decline as reaction temperature decreases.^{72–74}

We achieved the complete degradation of Vectra by methanolysis using 1.0 equiv of TBD under a reflux condition as the Vectra fibers totally disappeared. Accordingly, we focused on TBD for further studies at various TBD loadings, from 0.1 to 1.0 equiv relative to the ester bond in Vectra under reflux conditions. The final yields of **1a** and **2a** decreased with decreasing TBD loading (Figure 5b and Table S2, entries 1 and 3–5). This is consistent with the weight fractions of residual Vectra after 100 h (Figure 5c). These results suggested that TBD did not serve as a catalyst, and it was different from TBD-mediated degradation of other polyesters such as PET. The glycolysis of PET was completed in 8 min in the presence of 0.1 equiv of TBD.³¹

The yields almost reached the maximum at 30 h for all TBD loadings; for example, more than 95% of Vectra was degraded for 30 h under a reflux condition using 1.0 equiv of TBD. The ratio of **1a** to **2a** in the methanolysis products were almost constant at 7 to 3 throughout the reaction (Figure S4). We also studied the methanolysis using a larger amount of methanol (6.4 mL) (Table S2, entry 2). However, significant differences were not observed, probably due to the excess methanol, 146 and 200 equiv for 4.3 and 6.4 mL of methanol, respectively, relative to the ester bonds in Vectra. Compared with the degradation of other superengineering plastics, which requires high pressure, temperature, and excess reagents,^{49–52} this condition was significantly mild, efficient, and low energy consumption.

No oligomers were detected in the methanolysates in the supernatants under these heating conditions (Figure 6a). The treatment with Amberlyst 15 recovered **1a** and **2a** containing no TBD (Figure 6b). In addition, a few signals of **1a** and **2a** shifted slightly, and new peaks corresponding to their hydroxy groups appeared after removing TBD, which paradoxically supported the adducts formation between TBD and **1a/2a**. Attenuated total reflectance-Fourier-transform infrared (ATR-FTIR) spectra of Vectra and purified soluble methanolysis products indicated that the C=O stretching band shifted from 1724 to 1681 cm^{-1} and two new bands appeared at around 3418 and 3349 cm^{-1} after the degradation (Figure S5). This observation qualitatively supports the generation of monomeric methyl esters by the methanolysis and their high purity. The SEC and high-performance liquid chromatography (HPLC) chromatograms of the methanolysates showed peaks corresponding to a mixture of **1a** and **2a** (Figure S6). To the best of our knowledge, this is the first report on the degradation of wholly aromatic thermotropic LC polyesters to recover their corresponding monomeric compounds.

Compatibility of the material surface with solvents is important in heterogeneous reactions such as the degradation of poorly soluble polymers. Solvent polarity also affects the reactivities of substrates, reactants, and catalysts. The solvent effects were reported for the degradation of aromatic polyesters and polycarbonates.^{29,54–56} Thus, we examined toluene, tetrahydrofuran (THF), and acetonitrile as the solvent for the degradation of Vectra by adding 10 equiv of methanol and 0.1 equiv of TBD relative to the ester group of Vectra (Table S3). Due to the lower boiling point of THF than that of methanol, the reactions were conducted at 60 °C. The yields in methanolysis in toluene, THF, and acetonitrile were 26, 30, and 21%, respectively, which were higher than that (17%) for the simple methanolysis using methanol as the reaction medium (Table S3). A similar trend was observed in the degradation of PET and BPA-PC.^{28,54,55} Aromatic solvents having an electron-sufficient aromatic ring such as anisole were reported to interact with an electron-deficient aromatic ring of PET, which resulted in stabilization of the overall reaction energy in the glycolysis of PET.⁵⁵ On the other hand, THF was recently found to be a suitable solvent to promote swelling of the PET surface, which facilitated diffusion of the degradation media in the sample.⁷⁵ Similarly, toluene and THF may contribute to the high yields of **1a** and **2a** in the degradation of Vectra.

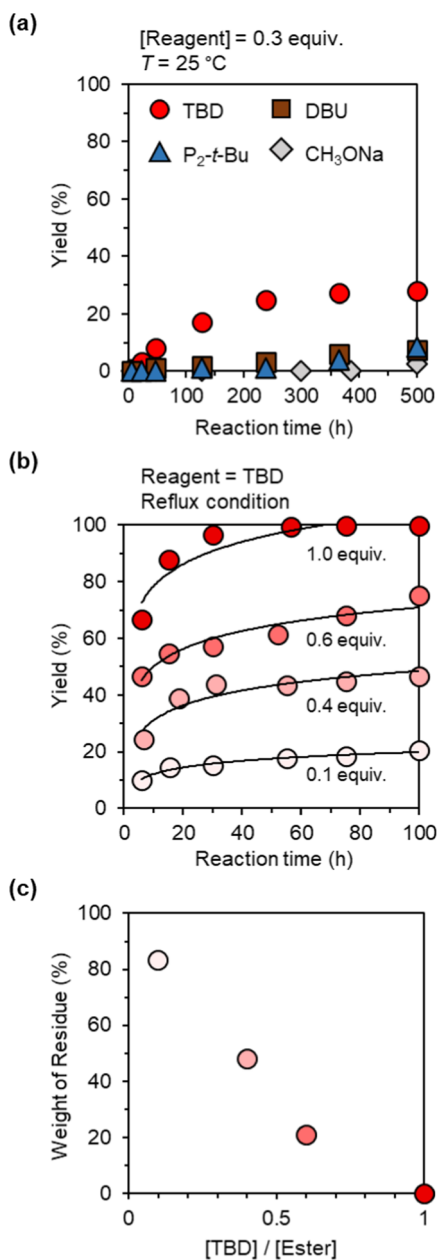


Figure 5. Degradation of Vectra under different conditions. Time courses of the yields of **1a** and **2a** in methanolysis using various bases (0.3 equiv) at 25 °C (a), and different TBD loadings under reflux conditions (b). Weight fractions of residual Vectra after 100 h of methanolysis as a function of the TBD loading (c).

2.2. Hydrolysis

Hydrolysis may be a more useful and acceptable degradation approach due to its lower environmental impact compared with solvolysis using organic solvents including methanol. Moreover, the resultant aromatic hydroxy acids can readily be used as monomeric precursors to Vectra.⁷ We examined the hydrolysis of Vectra using the organic bases and acids evaluated in the methanolysis, along with NaOH as the conventional base. The hydrolysis did not proceed effectively for any bases and acids (0.3 equiv relative to the ester group of Vectra) at 25 °C. The calculation of the yields of 4-hydroxybenzoic acid (**1b**) and 6-hydroxy-2-naphthoic acid (**2b**) was not applicable because of the low amount of hydrolysates dissolved in the supernatants.

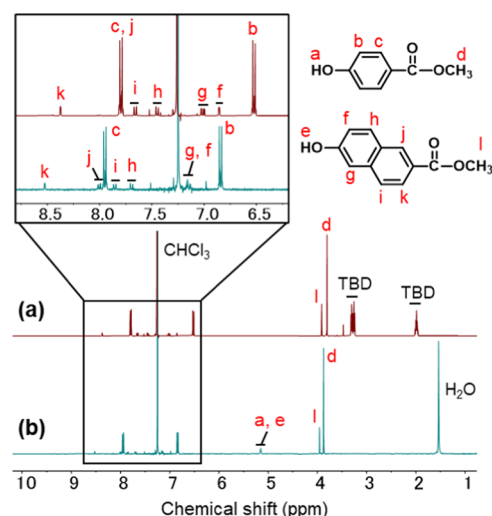


Figure 6. ¹H NMR spectrum (400 MHz in CDCl₃) of the supernatant in the methanolysis of Vectra using TBD (1.0 equiv) under a reflux condition for 100 h before (a) and after (b) treatment with Amberlyst 15.

Thus, high temperature conditions were examined to facilitate the hydrolysis of Vectra. Under reflux conditions, P₂-t-Bu marginally facilitated the hydrolysis with a yield of 7% after 75 h (Table S4, entry 1). These results were similar to those of our previous study of catalytic hydrolysis of poly(trimethylene carbonate), where P₂-t-Bu exhibited higher activity than other organic bases and acids.⁵⁷ This exceptional activity can be attributed to its strong basicity and possible stability in water.

We further studied the hydrolysis of Vectra under reflux conditions at various P₂-t-Bu loadings. The ¹H NMR spectra of the supernatants showed complex signals including those corresponding to **1b** and **2b** (Figure 2a, R = H) and minor undefined signals at 8.5–6.5 ppm, which corresponded to oligomers of **1b** and **2b** (Figure S7). The progress of the degradation was determined from the remaining weights of the residue at 100 h, which decreased with the base loading (Figure S8). We observed that more than 70% of Vectra underwent hydrolysis with 1.5 equiv of P₂-t-Bu for 100 h under reflux (Table S4, entry 4).

Vectra exhibited tolerance to hydrolysis in a buffer solution under alkali conditions.^{76,77} However, we observed that 26% of Vectra was degraded by the hydrolysis at 25 °C for 513 h in 1 M NaOH aqueous solution (NaOH = 4.8 equiv relative to the ester group of Vectra) using isopropanol as a cosolvent (Table S5, entry 4). When the hydrolysis was conducted with 0.3 equiv of NaOH, the yield was less than 1%, irrespective of the cosolvent and temperature (Table S4, entry 7 and Table S5, entries 1 and 2). These results indicate that P₂-t-Bu is more efficient than other bases and acids for promoting the hydrolysis of Vectra under moderate heating. Overviewing the reaction conditions and degrees of degradation, the methanolysis using TBD is more useful for the degradation of Vectra.

2.3. Mechanistic Insights on Degradation

The equimolar TBD was required to complete the methanolysis of Vectra in methanol; this was different from the TBD-catalyzed degradation of other polyesters and polycarbonate.^{31,33} These results implied that the base was deactivated by the degradates **1a** and **2a**. The results of the

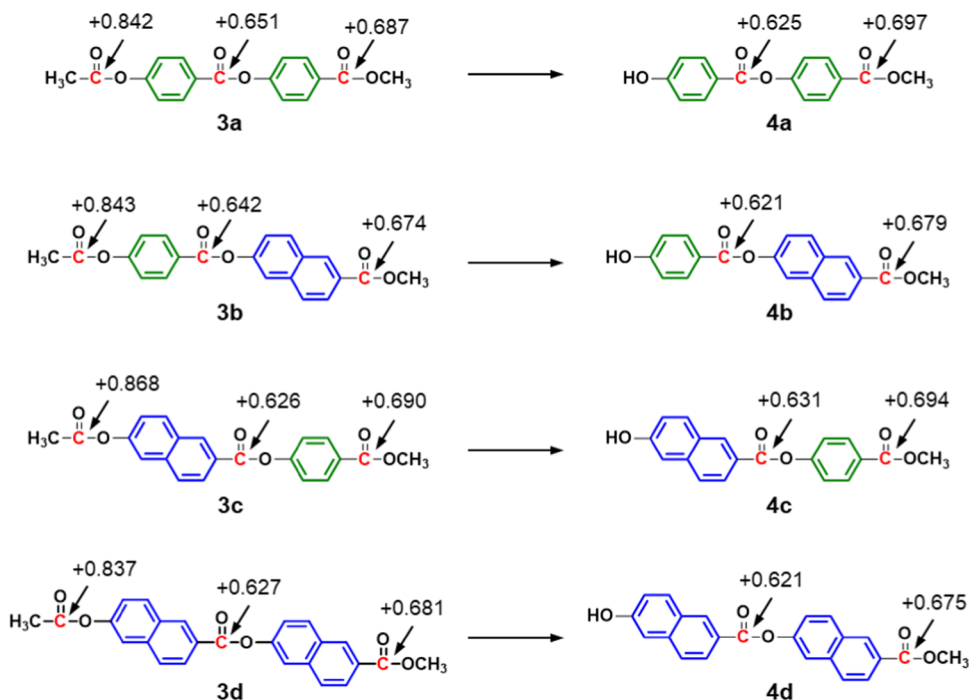


Figure 7. Electrostatic charges of the carbonyl carbon atoms in model aryl arylates **3a–d** and their deacetylated derivatives **4a–d** calculated using DFT.

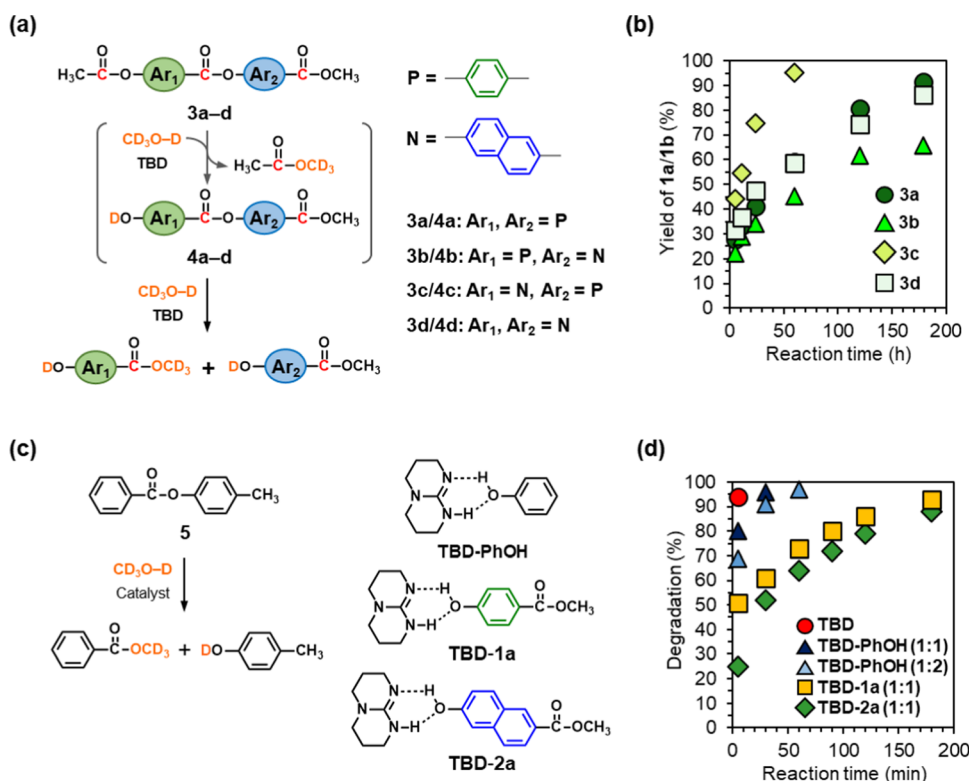


Figure 8. Model reactions for methanolysis of Vectra. (a, b) Methanolysis of aryl arylates **3a–d** at 25 °C mediated by TBD (0.4 equiv). (c, d) Methanolysis of *p*-tolyl benzoate (**5**) at 25 °C using TBD and its adducts (0.4 equiv). (a, c) Reaction schemes. (b, d) Time courses of the degrees of degradation of **3a–d** and **5**.

hydrolysis of Vectra was ascribed to the neutralization of the bases by the hydrolysates (**1b** and **2b**). Similarly, the acidic phenol structures of the methanolsates (**1a** and **2a**) formed adducts with the bases,⁵⁶ this was supported by the ¹H NMR spectra of **1a** and **2a** before and after the treatment with the

ion-exchange resin (Figure 6). We examined the methanolysis of Vectra using TBD (0.1 equiv) with tertiary amines (1.0 equiv) to avoid the formation of TBD-adducts with the degradates (Figure S9). However, the yields of the methanolsates did not increase, indicating the unavoidable

formation of TBD-adducts due to the weaker basicity of the tertiary amines than that of TBD. Acid–base complexes usually remain active when strong bases and acids are used while decreasing the activity, as TBD–acid salts were reported to catalyze the transesterification of PET.^{72–74} However, the inherent structure of Vectra could cause the inefficient degradation.

We estimated the electrostatic charges of the carbonyl carbons in the ester groups for four aryl arylate compounds (3a–d) consisting of 1a and 2a as the models of Vectra using density functional theory (DFT) calculation (Figure 7). The results revealed that aryl arylate structures were the least reactive because of the low values of positive charges on the carbonyl carbons. The order of electrophilicity of the carbonyl carbons was as follows: aryl acetate (+0.837 to +0.868) > methyl arylates (+0.674 to +0.690) > aryl arylates (+0.626 to +0.651). The calculation of atomic charges showed that the ester bonds in Vectra were inherently less reactive than those in PET.

We also synthesized the four model compounds 3a–d to examine the methanolysis using 0.4 equiv of TBD at 25 °C (Figure 8a). The reactions were conducted in CD₃OD for facile monitoring by ¹H NMR spectroscopy. The compounds 3a–d did not fully dissolve in CD₃OD, resulting in heterogeneous reactions. The progress of the reaction was examined by visual inspection and ¹H NMR spectroscopy (Figure S10). The methanolysis of 3c was almost completed, with more than 99% of degradation at 60 h, whereas those of 3a, 3b, and 3d took longer than 179 h to reach over 85% of degradation (Figure 8a,b). The methanolysates of 3a–d were also obtained as adducts with TBD (Figure S10). However, the degradation profiles of 3a–d were completely different from those of Vectra, where the profiles reached a plateau when a catalytic amount of TBD was used (Figure 5b). These results suggest that TBD is still active in the methanolysis of aryl arylates in heterogeneous systems even after the formation of the adducts with the methanolysates.

Among the model reactions, 3c was almost completely degraded (Figure 8a,b), which should be elucidated. The high values of the positive charges of the carbonyl carbons of the aryl acetate structures (Figure 7) suggest the deacetylation to form 4a–d as the first step of the model reactions. The carbonyl carbon atom of the acetyl group in 3c was the most electrophilic (+0.868, Figure 7). Furthermore, the calculation of the electrostatic charges of 4a–d suggested that the carbonyl carbon of the aryl arylate in 4c had the highest positive charge (+0.631, Figure 7). These results explain the specific reactivity of 3c during the methanolysis.

Subsequently, we examined the catalytic activities of TBD-adducts in methanolysis using a simple aryl arylate as a model for a homogeneous reaction. TBD-adducts with phenol, 1a, and 2a were prepared for the methanolysis of *p*-tolyl benzoate (5) dissolved in CD₃OD at 25 °C (Figure 8c). Unlike 3a–d, methanolysis proceeded faster and reached more than 90% of degradation for all TBD-adducts (0.4 equiv) after 200 min (Figure 8c,d). The reaction rates differed according to the acidity of the phenolic OH group of the original phenols; those of 1a and 2a were more acidic than that of phenol due to the electron-withdrawing ester substituent. These homogeneous model reactions revealed that the TBD-adducts with phenols remained sufficiently active as the transesterification catalysts in the methanolysis of the esters dissolved in solution. In addition, high catalytic activities of these adducts in

homogeneous methanolysis supported the presence of 1a and 2a as major degradates in supernatants in the methanolysis of Vectra (Figure 6).

The results of the two model reactions (Figure 8) suggest that the poor solubility of the substance and the adduct formation are responsible for the inefficiency in the methanolysis of Vectra using TBD. There may be a significant difference in the activity between fresh TBD and the TBD-adducts.⁷⁸ Two activation mechanisms were proposed for transesterification using TBD: dual hydrogen bonding and acyl transfer (Figure S2).^{31,71} The former includes dual activation of the ester C=O and alcohol O–H by N–H as a hydrogen bond donor and imine nitrogen as a hydrogen bond acceptor, respectively. The close geometry of the activated C=O and O–H drives the reaction. The latter begins with nucleophilic attack to the ester carbonyl by the imine nitrogen of TBD to form an acyl-TBD adduct, which undergoes nucleophilic attack by an alcohol to form another ester and regenerate TBD. In both cases, the mechanisms are specific to TBD, not TBD-adducts. The specific catalysis of TBD is considered to be crucial for cleavage of the ester bonds of Vectra in the heterogeneous reaction system.

2.4. Solid-State Structure of Residual Vectra in Methanolysis

The residues after the methanolysis of Vectra were examined with optical microscopy, scanning electron microscopy (SEM), X-ray diffraction (XRD) measurement, differential scanning calorimetry (DSC), thermogravimetry (TG), and ATR-FTIR spectroscopy. The residual Vectra at different degrees of degradation were analyzed to study the degradation mechanism of Vectra. The residual Vectra with 47 and 75% of degradation were obtained by filtering the reaction mixtures of methanolysis for 100 h under reflux conditions using 0.4 and 0.6 equiv of TBD, respectively (Figure 5b,c).

Optical micrographs and SEM images of pristine Vectra indicated fiber forms with widths of approximately 30 μm (Figure 9a, left, center). The Vectra fibers transformed into powders after the methanolysis using 0.6 equiv of TBD (Figure 3). The optical microscopy revealed that the residual Vectra treated with 0.6 equiv of TBD comprised short fibers with lengths of less than 200 μm (Figure 9c, left). The SEM images showed a smooth fiber surface for pristine Vectra, while the surface became rougher after 47% degradation (Figure 9b, center, right). Finally, several cracks were formed parallel to the fiber axis at 75% degradation (Figure 9c, center, right). Sawyer and Jaffe studied the morphology of uniaxially oriented extrudates of a thermotropic LC copolyester composed of 1,4-phenylene and 2,6-naphthalene structures.⁷⁹ They revealed that the oriented polyester possessed a hierarchical structure composed of fibrillar subunits with diameters ranging from several nanometers to micrometers along the fiber axis. The morphological changes observed in the present study suggest that Vectra fibers are degraded by the surface erosion mechanism, preferentially from less ordered regions.

XRD profile of the residual Vectra with 75% degradation was compared with that of pristine Vectra (Figure 10). The profile of pristine Vectra was recorded by irradiating the fibers placed radially on a substrate to exclude the effect of chain orientation. The profile of pristine Vectra showed peaks at $2\theta = 19.6$ and 27.7° , which corresponded well with that of a powder of Vectra, prepared by milling an extruded sample.⁸⁰ After the degradation, additional peaks appeared at $2\theta = 23.9^\circ$.

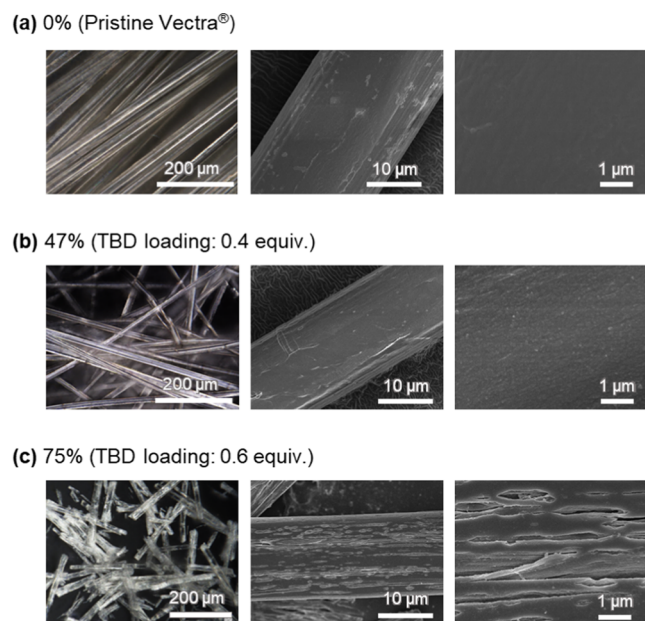


Figure 9. Optical micrographs and SEM images of the residual Vectra at different degrees of degradation: (a) 0% (b) 47%, and (c) 75%. Methanolysis was conducted for 100 h under reflux using different equivalents of TBD. The degrees of degradation were calculated based on the yields of **1a** and **2a** dissolved in the supernatants.

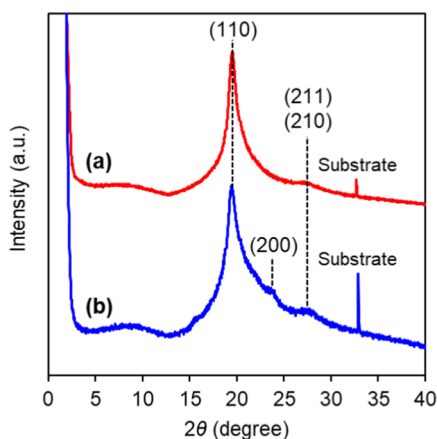


Figure 10. Normalized XRD profiles of pristine and residual Vectra at 28 °C. (a) Pristine Vectra fiber. (b) Residual Vectra powder with 75% degradation. Each peak is characterized with respect to an orthorhombic lattice.

A similar change in the XRD profiles was characterized to a polymorphic transformation from pseudo-hexagonal to orthorhombic lattices.^{81–83} However, these changes were induced by annealing at 200 °C and above. The pseudo-hexagonal lattice has a less chain-packed structure than the orthorhombic lattice.⁸⁴ This structure may facilitate penetration of degradation media into the samples. In the present study, the change of the XRD profiles was ascribed to the preferential degradation of the pseudo-hexagonal structure, increasing the fraction of the orthorhombic structure, which was a minority in pristine Vectra (Figure 10). Moreover, the peak at 19.8° appeared to be broaden slightly after the degradation, suggesting a low degree of order of the polymer chain (Figure S11). Given that the polymer chain is highly oriented at the surface,^{8,80} this change in the XRD profile was ascribed to the

decrease in the well-ordered fraction at the surface, supporting the surface erosion as a degradation mechanism.

DSC thermograms of both pristine and residual Vectra showed an endothermic peak at 310 °C as well as a broad endotherm in the range of 170–270 °C (Figure S12a).^{85,86} In addition, their TG curves were similar (Figure S12b). These observations suggested that there were no significant changes in the molecular structure and weight due to the methanolysis. The ATR-FTIR spectrum of the residual Vectra was similar to that of pristine Vectra except for the C=O stretching band of the ester bond (1725 and 1731 cm^{-1} for pristine and residual Vectra, respectively) (Figure S12c).⁸⁷ These results highlight the stability of the chemical structure of Vectra. Due to the poor solubility, solution analyses such as NMR and SEC are not applicable to pristine and residual Vectra. Polymer chains of Vectra undergo orientation during the drawing process, which forms a robust structure over the attack by nucleophiles such as methanol and water, even if activated by the superbases.

3. CONCLUSIONS

We found that organic superbases such as TBD substantially mediated the methanolysis of a wholly aromatic main-chain thermotropic LC polymer, Vectra under heating conditions. The degradates were obtained as monomeric units. The monomeric units of Vectra as the degradates contained phenolic OH, which deteriorated the basicity of the superbases by forming adducts. The DFT calculation suggested that the ester group in the aryl arylate structures were less reactive than those in the alkyl arylate and the aryl alkylate structures. The model reactions using small molecules containing aryl arylate structures exhibited a decrease in the reactivity of the ester groups in the heterogeneous systems. Microscopic observation and XRD analysis of the residual Vectra revealed that the solvolysis of Vectra proceeded via the surface erosion mechanism, preferentially starting from the less chain-packed regions. The robust oriented structure enhanced the ester bonds in Vectra compared with other polyesters in the heterogeneous reaction. By the specific mechanisms along with the strong basicity, only TBD could mediate the methanolysis of Vectra. These results pave the way for recycling high-performance plastics and demonstrate the feasibility of recovering precious aromatic compounds from plastic waste as aromatic feedstock.^{49–53,88}

4. EXPERIMENTAL SECTION

4.1. Materials

Vectra, a wholly aromatic main-chain thermotropic LC polyester, was obtained as a fiber form with a diameter of 0.023 mm from GoodFellow Cambridge Ltd. (Cambridge, England). 4-Acetoxybenzoic acid, 6-acetoxy-2-naphthoic acid, 1,8-bis(dimethylamino)-naphthalene (proton sponge), 1,8-diazabicyclo[5.4.0]-7-undecene (DBU), 4-dimethylaminopyridine (DMAP), 1-(3-(dimethylamino)propyl)-3-ethylcarbodiimide hydrochloride (EDC-HCl), methyl 4-hydroxybenzoate, methyl 6-hydroxy-2-naphthoate, phenol (PhOH), *p*-toluenesulfonic acid monohydrate, *p*-tolyl benzoate, and 1,5,7-triazabicyclo[4.4.0]dec-5-ene (TBD) were obtained from Tokyo Chemical Industry (TCI) (Tokyo, Japan). Amberlyst 15 proton form, 1-*tert*-butyl-2,2,4,4,4-pentakis(dimethylamino)-2 Λ^3 ,4 Λ^5 -catenadi(phosphazene) (P_2 -*t*-Bu) in THF (~2 M), methanesulfonic acid (MSA), sodium hydroxide, triethylamine (Et_3N), and trifluoromethanesulfonic acid (TfOH) were purchased from Sigma-Aldrich (Tokyo, Japan). Sodium methoxide and zinc acetate were purchased

from Fujifilm Wako Pure Chemical (Tokyo, Japan). All chemicals were used as received.

4.2. Measurement

¹H NMR spectra were acquired on JEOL JNM-ECX400 operated at a frequency of 400 MHz. CD₃OD and CDCl₃ were used as solvents containing tetramethylsilane (TMS) as an internal standard. SEC was conducted at 40 °C on an integrated SEC unit of HLC-8420 EcoSEC Elite equipping refractive index and UV detectors (UV-8420) and two TSK-gel columns. THF was used as an eluent. TSK-gel column SuperMultiporeHZ-M was employed for the measurements. TG was conducted on a Rigaku TG-DTA 8122 in N₂ atmosphere at the rate of 5 °C min⁻¹. DSC was carried out in N₂ atmosphere at the rate of 5 °C min⁻¹ using a NETZSCH DSC3500 Series. XRD patterns were recorded on a Rigaku SmartLab equipped with a hot stage using nickel-filtered Cu K α radiation (1.54 Å) at room temperature (~25 °C). Silicon wafers were used as substrates for the XRD measurements. HPLC was conducted at 30 °C in methanol with a flow rate of 1 mL min⁻¹ using a Shimadzu LC-2050C 3D equipped with Shim-pack Scepter C18–120. Optical microscope observation was performed using a KEYENCE digital microscope VHX970FN. SEM was conducted using a JEOL JSM-7500FA, operating at an acceleration voltage of 3.0 kV. The samples were mounted on a substrate using a carbon adhesive tape and coated with osmium in advance. ATR-FTIR spectra were recorded on JASCO/FTIR-660 Plus spectrometer with ATR accessories. Atomic charges of compounds were calculated by DFT using Spartan'18.

4.3. Synthesis

4.3.1. 3,4,6,7,8,9-Hexahydro-2H-pyrimido[1,2-*a*]pyrimidin-1-ium *p*-Toluenesulfonate (TBD-PTSA). TBD-PTSA was synthesized as described elsewhere.⁷² In a 50 mL vial, TBD (0.70 g, 5.0 mmol) was dissolved in acetone (10 mL) and mixed with *p*-toluenesulfonic acid monohydrate (0.95 g, 5.0 mmol) in acetone (10 mL). The mixture was stirred for 1 h at 60 °C in an argon atmosphere. The solution was allowed to cool to room temperature (20–25 °C) and poured into Et₂O (60 mL). The precipitated solid was collected by filtration and dried in vacuum to give TBD-PTSA as a white solid (1.4 g, 92%). ¹H NMR (CDCl₃, 400 MHz): δ 8.56 (s, 2H, OH, NH), 7.92–7.71 (m, 2H, Ar-H), 7.23–7.12 (m, 2H, Ar-H), 3.40–3.20 (m, 8H, CH₂), 3.01 (s, 3H, CH₃), 2.06–1.95 (m, 4H, CH₂).

4.3.2. 3,4,6,7,8,9-Hexahydro-2H-pyrimido[1,2-*a*]pyrimidin-1-ium Methanesulfonate (TBD-MSA). TBD-MSA was synthesized as described elsewhere.⁷³ In a 50 mL vial, TBD (1.0 g, 7.2 mmol) was dissolved in acetone (10 mL) and mixed with MSA (0.69 g, 7.2 mmol) in acetone (10 mL). The mixture was stirred for 1 h at 60 °C in argon atmosphere. The solution was allowed to cool to room temperature (20–25 °C) and stored in a refrigerator (~4 °C). A precipitated solid was collected by filtration and dried in vacuum to give TBD-MSA as a white solid (1.2 g, 71%). ¹H NMR (CDCl₃, 400 MHz): δ 8.54 (s, 2H, OH, NH), 3.36–3.26 (m, 8H, CH₂), 2.83 (s, 3H, CH₃), 2.08–1.93 (m, 4H, CH₂).

4.3.3. 4-(Methoxycarbonyl)phenyl 4-Acetoxybenzoate (3a). 4-Acetoxybenzoic acid (0.99 g, 5.5 mmol), methyl 4-hydroxybenzoate (0.70 g, 4.6 mmol), EDC-HCl (1.3 g, 6.7 mmol), and DMAP (0.083 g, 0.70 mmol) were mixed in CH₂Cl₂ (185 mL) and stirred for 21 h at room temperature (20–25 °C) in an argon atmosphere. The reaction mixture was washed with distilled water (2 × 100 mL) and brine (100 mL), and dried over MgSO₄. After the removal of the salt by filtration, the filtrate was concentrated under reduced pressure. The residue was recrystallized from a mixture of chloroform and ethanol to give 3a as a white powder (0.73 g, 50%). ¹H NMR (CDCl₃, 400 MHz): δ 8.27–8.09 (m, 4H, Ar-H), 7.34–7.23 (m, 4H, Ar-H), 3.93 (s, 3H, COOCH₃), 2.35 (s, 3H, CH₃). ¹³C NMR (CDCl₃, 100 MHz): δ 168.9, 166.5, 164.0, 155.2, 154.7, 132.1, 132.0, 131.4, 128.0, 126.8, 122.1, 121.9, 52.4. Elemental analysis (%) calcd for C₁₇H₁₄O₆: C 64.97, H: 4.49; found: C 64.83, H 4.31.

4.3.4. Methyl 6-((4-Acetoxybenzoyl)oxy)-2-naphthoate (3b). 4-Acetoxybenzoic acid (1.0 g, 5.6 mmol), methyl 6-hydroxy-2-naphthoate (0.94 g, 4.7 mmol), EDC-HCl (1.3 g, 6.7 mmol), and

DMAP (0.083 g, 0.68 mmol) were mixed in CH₂Cl₂ (185 mL) and stirred for 7 h at room temperature (20–25 °C) in an argon atmosphere. The reaction mixture was washed with distilled water (2 × 100 mL) and brine (100 mL), and dried over MgSO₄. After the removal of the salt by filtration, the filtrate was concentrated under reduced pressure. The residue was recrystallized from a mixture of chloroform and ethanol to give 3b as a white powder (1.14 g, 67%). ¹H NMR (CDCl₃, 400 MHz) δ 8.70–7.20 (m, 10H, Ar-H), 4.00 (s, 3H, COOCH₃), 2.36 (s, 3H, CH₃). ¹³C NMR (CDCl₃, 100 MHz) δ 168.8, 167.1, 164.3, 155.0, 150.4, 136.1, 131.9, 131.0, 130.9, 130.6, 128.0, 127.5, 126.8, 126.1, 122.1, 122.0, 118.7, 52.3, 21.2. Elemental analysis (%) calcd for C₂₁H₁₆O₆: C 69.23, H 4.43; found: C 69.20, H 4.39.

4.3.5. Methyl 4-(Methoxycarbonyl)phenyl 6-Acetoxy-2-naphthoate (3c). 6-Acetoxy-2-naphthoic acid (1.3 g, 5.6 mmol), methyl 4-hydroxybenzoate (0.70 g, 4.6 mmol), EDC-HCl (1.3 g, 6.7 mmol), and DMAP (0.083 g, 0.68 mmol) were mixed in CH₂Cl₂ (185 mL) and stirred for 16 h at room temperature (20–25 °C) in an argon atmosphere. The reaction mixture was washed with distilled water (2 × 100 mL) and brine (100 mL), and dried over MgSO₄. After the removal of the salt by filtration, the filtrate was concentrated under reduced pressure. The residue was recrystallized from a mixture of chloroform and ethanol to give 3c as a white powder (1.07 g, 64%). ¹H NMR (CDCl₃, 400 MHz) δ 8.90–7.30 (m, 10H, Ar-H), 3.95 (s, 3H, COOCH₃), 2.39 (s, 3H, CH₃). ¹³C NMR (CDCl₃, 100 MHz) δ 169.5, 166.5, 164.8, 154.8, 150.8, 136.7, 132.0, 131.4, 131.2, 130.6, 128.4, 128.0, 126.4, 126.3, 122.6, 121.9, 118.8, 52.4, 21.4. Elemental analysis (%) calcd for C₂₁H₁₆O₆: C 69.23, H 4.43; found: C 68.70, H 4.33.

4.3.6. 6-(Methoxycarbonyl)naphthalen-2-yl 6-Acetoxy-2-naphthoate (3d). 6-Acetoxy-2-naphthoic acid (1.3 g, 5.6 mmol), methyl 6-hydroxy-2-naphthoate (0.94 g, 4.7 mmol), EDC-HCl (1.3 g, 6.7 mmol), and DMAP (0.084 g, 0.69 mmol) were mixed in CH₂Cl₂ (185 mL) and stirred for 17 h at room temperature (20–25 °C) in an argon atmosphere. The reaction mixture was washed with distilled water (2 × 100 mL) and brine (100 mL), and dried over MgSO₄. After the removal of the salt by filtration, the filtrate was concentrated under reduced pressure. The residue was recrystallized from a mixture of chloroform and ethanol to give 3d as a white powder (1.8 g, 93%). ¹H NMR (CDCl₃, 400 MHz) δ 8.90–7.30 (m, 12H, Ar-H), 4.00 (s, 3H, COOCH₃), 2.40 (s, 3H, CH₃). ¹³C NMR (CDCl₃, 100 MHz) δ 169.5, 167.2, 165.3, 150.7, 150.7, 136.6, 136.3, 132.0, 131.3, 131.2, 131.0, 130.7, 130.6, 128.4, 128.1, 127.6, 126.6, 126.3, 126.2, 122.6, 122.4, 118.9, 118.8, 52.4, 21.4. Elemental analysis (%) calcd for C₂₅H₁₈O₆: C 72.46, H 4.38; found: C 72.15, H 4.27.

4.3.7. TBD-1a. In a 12 mL vial, TBD (0.71 g, 5.1 mmol) and methyl 4-hydroxybenzoate (0.76 g, 5.0 mmol) were mixed in methanol (5.0 mL) and stirred for 24 h at room temperature. The solution was concentrated and dried in vacuum to give TBD-1a as a white solid. ¹H NMR (CDCl₃, 400 MHz) δ 7.82–7.76 (m, 2H, Ar-H), 6.55–6.47 (m, 2H, Ar-H), 3.80 (s, 3H, CH₃), 3.37–3.17 (m, 8H, CH₂), 2.02–1.94 (m, 4H, CH₂).

4.3.8. TBD-2a. In a 12 mL vial, TBD (0.71 g, 5.1 mmol) and methyl 6-hydroxy-2-naphthoate (1.0 g, 5.0 mmol) were mixed in methanol (6.0 mL) and stirred for 24 h at room temperature. The solution was concentrated and dried in vacuum to give TBD-2a as a white solid. ¹H NMR (CDCl₃, 400 MHz) δ 8.38 (d, *J* = 1.5 Hz, 1H, Ar-H), 7.80 (dd, *J* = 8.6, 1.8 Hz, 1H, Ar-H), 7.67 (d, *J* = 9.0 Hz, 1H, Ar-H), 7.46 (d, *J* = 8.8 Hz, 1H, Ar-H), 7.05 (dd, *J* = 8.8, 2.5 Hz, 1H, Ar-H), 6.91 (d, *J* = 2.3 Hz, 1H, Ar-H), 3.91 (s, 3H, CH₃), 3.28 (t, *J* = 5.8 Hz, 4H, CH₂), 3.21 (t, *J* = 5.9 Hz, 4H, CH₂), 2.01–1.88 (m, 4H, CH₂).

4.4. Degradation

4.4.1. Methanolysis. **4.4.1.1. General Procedure Using Methanol as a Solvent.** In a 2 mL-vial, Vectra (50 mg, ester group = 0.38 mmol) and a catalyst (0.11 mmol, 0.3 equiv) in methanol (1.8 mL) were charged and stirred at 25 °C. The aliquots (100 μ L) were taken from the supernatant at a predetermined time to monitor the progress of the reactions by ¹H NMR and SEC.

For heating conditions, Vectra (100 mg, ester group = 0.75 mmol) and TBD in methanol (4.3 mL) were charged in a 30 mL Schlenk tube. The mixture was stirred and heated by an aluminum block with a preset temperature of 73 °C. Aliquots (50 μ L) taken at a predetermined time were examined by ^1H NMR and SEC. The unreacted residues after 100 h were collected by filtration and dried in vacuum for the subsequent characterizations.

4.4.1.2. General Procedure Using Other Solvents. Toluene, acetonitrile, and THF were used as solvents. Vectra (100 mg, ester group = 0.75 mmol) and TBD (0.11 mmol, 0.1 equiv) in a solvent (4.0 mL) with methanol (0.3 mL, 10 equiv) were charged in a 12 mL vial. The reaction mixture was stirred and heated by an oil bath with a preset temperature of 60 °C. The aliquots (50 μ L) were taken from the supernatant at a predetermined time to monitor the progress of reactions.

4.4.1.3. General Procedure Using Tertiary Amines. Vectra (100 mg, ester group = 0.75 mmol), TBD (0.11 mmol, 0.1 equiv), and a tertiary amine (0.75 mmol, 1 equiv) in methanol (4.3 mL) were charged in a 30 mL Schlenk tube. The mixture was stirred and heated by an aluminum block with a preset temperature of 73 °C. The aliquots (50 μ L) were taken from the supernatant at a predetermined time to monitor the progress of reactions.

4.4.1.4. Purification of Methanolysates. The residue and the supernatant were separated by filtration. The residual Vectra was rinsed with methanol and dried in vacuum for SEM, XRD, TG, and DSC. The filtrates were treated with Amberlyst 15 to remove the base, concentrated, and dried in vacuum for characterizations with ^1H NMR, SEC and HPLC.

4.4.1.5. Model Reactions Using 3a–d. In 2-mL vials, 3a–d (0.17 mmol), TBD (0.07 mmol, 0.4 equiv relative to 3a–d), and CD_3OD (1.0 mL) were charged and stirred at 25 °C. Aliquots (30 μ L) of the supernatants were taken at several time points to monitor the progress of the degradation by ^1H NMR.

4.4.1.6. Model Reactions Using *p*-Tolyl Benzoate (5). In 6-mL vials, 5 (0.16 g, 0.75 mmol), adducts of TBD (TBD-1a, TBD-2a, and TBD-PhOH, 0.30 mmol, 0.4 equiv), and CD_3OD (4.3 mL) were charged and stirred at 25 °C. Aliquots (100 μ L) of the mixtures were taken at several time points to monitor the progress of the degradation by ^1H NMR. The TBD-PhOH adduct was prepared in the reaction mixture before adding 5 as the adduct was sublimable.

4.4.2. Hydrolysis. The protocol was the same as the methanolysis at 25 °C. Distilled water was used as a solvent instead of methanol. For a mixed solvent condition, isopropanol (IPA) was used as a cosolvent. The volume ratio of water to IPA was 7 to 3.

For the reaction at high temperature, the protocol was similar to that of the methanolysis at 73 °C. Distilled water was used instead of methanol and the preset temperature of the aluminum block was 113 °C.

4.4.3. Calculation of Percentages of Degradation. Yields of the monomeric units were calculated as $n_d/n_p \times 100$ (%), where n_d and n_p are molar amounts of monomeric degradates in supernatants and Vectra initially loaded (calculated as a monomer unit), respectively. The n_d was estimated by the integral ratios of the degradates and TBD (or $(\text{CH}_3)_2\text{SO}_2$) in ^1H NMR spectrum. Weight fractions of the residual Vectra were calculated by $W_t/W_0 \times 100$ (%), where W_0 and W_t represent the initial weight of Vectra and the weight of the residual Vectra, respectively.

4.5. Calculation of Atomic Charges

Atomic charges were obtained from a B3LYP/6-31G* density functional calculation. The calculation was conducted in a polar solvent ($\epsilon = 37$). This dielectric constant is the closest option in the software to that of methanol ($\epsilon = 26$ at 60 °C).⁸⁹

ASSOCIATED CONTENT

Supporting Information

The Supporting Information is available free of charge at <https://pubs.acs.org/doi/10.1021/jacsau.4c00286>.

Materials, experimental details, weight fractions of the residues after degradation, time courses of yields of the monomeric esters, NMR spectra, SEC profiles, HPLC chromatograms, XRD profiles, DSC thermograms, TG curves, and ATR-FTIR spectra (PDF)

AUTHOR INFORMATION

Corresponding Authors

Kazuki Fukushima – Department of Chemistry and Biotechnology, School of Engineering, The University of Tokyo, Tokyo 113-8656, Japan; Japan Science and Technology Agency (JST), PRESTO, Kawaguchi, Saitama 332-0012, Japan; orcid.org/0000-0002-6980-9663; Email: k_fukushima@chembio.t.u-tokyo.ac.jp

Takashi Kato – Department of Chemistry and Biotechnology, School of Engineering, The University of Tokyo, Tokyo 113-8656, Japan; Research Initiative for Supra-Materials, Shinshu University, Nagano 380-8553, Japan; orcid.org/0000-0002-0571-0883; Email: kato@chiral.t.u-tokyo.ac.jp

Author

Yuya Watanabe – Department of Chemistry and Biotechnology, School of Engineering, The University of Tokyo, Tokyo 113-8656, Japan; orcid.org/0000-0001-8250-3258

Complete contact information is available at: <https://pubs.acs.org/doi/10.1021/jacsau.4c00286>

Author Contributions

The manuscript was written through contributions of all authors. All authors have given approval to the final version of the manuscript.

Notes

The authors declare no competing financial interest.

ACKNOWLEDGMENTS

This study was supported by JSPS KAKENHI grants (JP19H05714, JP19H05715, and JP19H05716), JST PRESTO grant (JPMJPR21N7), and JST SPRING grant (JPMJSP2108). A part of this study was supported by “Advanced Research Infrastructure for Materials and Nanotechnology in Japan (ARIM)” of the Ministry of Education, Culture, Sports, Science and Technology (MEXT) (JPMXP1223UT-0199). The authors are grateful to Dr. Takanori Iwasaki and Dr. Junya Uchida of The University of Tokyo for valuable discussion and helpful advice.

ABBREVIATIONS

ATR-FTIR, attenuated total reflectance-Fourier-transform infrared; BPA-PC, bisphenol A polycarbonate; DBU, 1,8-diazabicyclo[5.4.0]undec-7-ene; DFT, density functional theory; DMAP, 4-dimethylaminopyridine; DSC, differential scanning calorimetry; EDC-HCl, 1-(3-(dimethylamino)propyl)-3-ethylcarbodiimide hydrochloride; HPLC, high performance liquid chromatography; LC, liquid-crystalline; MSA, methanesulfonic acid; NMR, nuclear magnetic resonance; PET, poly(ethylene terephthalate); PhOH, phenol; P_2 -*t*-Bu, 1-*tert*-butyl-2,2,4,4,4-pentakis-(dimethylamino)-2 Λ^5 ,4- Λ^5 -catenadi(phosphazene); SEC, size exclusion chromatography; TBD, 1,5,7-triazabicyclo-[4.4.0]dec-5-ene; TBD-PTSA, 3,4,6,7,8,9-hexahydro-2H-pyrimido[1,2-*a*]pyrimidin-1-ium *p*-

toluenesulfonate; TBD-MSA, 3,4,6,7,8,9-hexahydro-2H-pyrimido[1,2-a]pyrimidin-1-ium methanesulfonate; TfOH, trifluoromethanesulfonic acid; TG, thermogravimetry; THF, tetrahydrofuran; UV, ultraviolet; XRD, X-ray diffraction

REFERENCES

- (1) Greiner, A.; Schmidt, H.-W. Aromatic Main-Chain Liquid-Crystalline Polymers. In *Handbook of Liquid Crystals*; Goodby, J.; Collings, P. J.; Kato, T.; Tschierske, C.; Gleeson, H.; Raynes, P., Eds.; Wiley-VCH, 2014; pp 303–329.
- (2) Uchida, J.; Soberats, B.; Gupta, M.; Kato, T. Advanced Functional Liquid Crystals. *Adv. Mater.* **2022**, *34* (23), No. 2109063.
- (3) Kato, T.; Uchida, J.; Ichikawa, T.; Soberats, B. Functional Liquid-Crystalline Polymers and Supramolecular Liquid Crystals. *Polym. J.* **2018**, *50*, 149–166.
- (4) Kato, T.; Yoshio, M.; Ichikawa, T.; Soberats, B.; Ohno, H.; Funahashi, M. Transport of Ions and Electrons in Nanostructured Liquid Crystals. *Nat. Rev. Mater.* **2017**, *2*, No. 17001.
- (5) Jackson, W. J.; Kuhfuss, H. F. Liquid Crystal Polymers. I. Preparation and Properties of *p*-Hydroxybenzoic Acid Copolyesters. *J. Polym. Sci., Polym. Chem. Ed.* **1976**, *14* (8), 2043–2058.
- (6) Cottis, S. G. C.; Economy, J.; Wohrer, L. C. Process for Spinning High Modulus Oxybenzoyl Copolyester Fibers. US3975487, 1976.
- (7) Calundann, G. W. Polyester of 6-Hydroxy-2-Naphthoic Acid and *para*-Hydroxybenzoic Acid Capable of Readily Undergoing Melt Processing. US4161470, 1979.
- (8) Yoon, H. N.; Charbonneau, L. F.; Calundann, G. W. Synthesis, Processing and Properties of Thermotropic Liquid-Crystal Polymers. *Adv. Mater.* **1992**, *4* (3), 206–214.
- (9) MacDonald, W. A. Thermotropic Main Chain Liquid Crystal Polymers. In *Liquid Crystal Polymers: From Structures to Applications*; Elsevier, 1992; pp 407–446.
- (10) Cadogan, D.; Sandy, C.; Grahne, M. Development and Evaluation of the Mars Pathfinder Inflatable Airbag Landing System. *Acta Astronaut.* **2002**, *50* (10), 633–640.
- (11) Said, M. A.; Dingwall, B.; Gupta, A.; Seyam, A. M.; Mock, G.; Theyson, T. Investigation of Ultra Violet (UV) Resistance for High Strength Fibers. *Adv. Space Res.* **2006**, *37* (11), 2052–2058.
- (12) Ji, Y.; Bai, Y.; Liu, X.; Jia, K. Progress of Liquid Crystal Polyester (LCP) for 5G Application. *Adv. Ind. Eng. Polym. Res.* **2020**, *3* (4), 160–174.
- (13) Jackson, W. J. Liquid Crystal Polymers. IV. Liquid Crystalline Aromatic Polyesters. *Br. Polym. J.* **1980**, *12* (4), 154–162.
- (14) Ober, C.; Jin, J. I.; Lenz, R. W. Liquid Crystal Polymers. V. Thermotropic Polyesters with Either Dyad or Triad Aromatic Ester Mesogenic Units and Flexible Polymethylene Spacers in the Main Chain. *Polym. J.* **1982**, *14* (1), 9–17.
- (15) Galli, G.; Chiellini, E.; Ober, C. K.; Lenz, R. W. Liquid Crystalline Polymers. 8. Structurally Ordered Thermotropic Polyesters of Glycol Ethers. *Makromol. Chem.* **1982**, *183* (11), 2693–2708.
- (16) Chiellini, E.; Galli, G.; Malanga, C.; Spassky, N. Chiral Liquid Crystal Polymers. 3. Structurally Ordered Thermotropic Polyesters of Optically Active Propyleneglycol Ethers. *Polym. Bull.* **1983**, *9* (6–7), 336–343.
- (17) Zhou, Q.-F.; Lenz, R. W. Liquid Crystal Polymers. 15. Synthesis and Liquid Crystalline Properties of Alkyl-Substituted Polyesters. *J. Polym. Sci., Polym. Chem. Ed.* **1983**, *21* (11), 3313–3320.
- (18) Uryu, T.; Kato, T. Solid-State Cross Polarization/Magic Angle Spinning ^{13}C NMR Study of Thermotropic Aromatic Polyester Containing a Flexible Spacer in the Main Chain. *Macromolecules* **1988**, *21* (2), 378–384.
- (19) Kato, T.; Kabir, G. M. A.; Uryu, T. Solid-state CP/MAS ^{13}C -NMR Studies of Naphthalene-Based Thermotropic Polyesters and Model Compounds. *J. Polym. Sci., Part A: Polym. Chem.* **1989**, *27* (5), 1447–1465.
- (20) Goring, P. D.; Priestley, R. D. Polymer Recycling and Upcycling: Recent Developments toward a Circular Economy. *JACS Au* **2023**, *3* (10), 2609–2611.
- (21) Barnard, E.; Rubio Arias, J. J.; Thielemans, W. Chemolytic Depolymerization of PET: A Review. *Green Chem.* **2021**, *23* (11), 3765–3789.
- (22) Ragaert, K.; Delva, L.; Van Geem, K. Mechanical and Chemical Recycling of Solid Plastic Waste. *Waste Manage.* **2017**, *69*, 24–58.
- (23) Nair, L. S.; Laurencin, C. T. Biodegradable Polymers as Biomaterials. *Prog. Polym. Sci.* **2007**, *32* (8–9), 762–798.
- (24) Siracusa, V.; Rocculi, P.; Romani, S.; Rosa, M. D. Biodegradable Polymers for Food Packaging: A Review. *Trends Food Sci. Technol.* **2008**, *19* (12), 634–643.
- (25) Wang, G. X.; Huang, D.; Ji, J. H.; Völker, C.; Wurm, F. R. Seawater-Degradable Polymers—Fighting the Marine Plastic Pollution. *Adv. Sci.* **2021**, *8* (1), No. 2001121.
- (26) Carta, D.; Cao, G.; D'Angeli, C. Chemical Recycling of Poly(ethylene terephthalate) (PET) by Hydrolysis and Glycolysis. *Environ. Sci. Pollut. Res.* **2003**, *10* (6), 390–394.
- (27) Tong, S. N.; Chen, D. S.; Chen, C. C.; Chung, L. Z. Unsaturated Polyesters Based on Bis(2-hydroxyethyl)terephthalate. *Polymer* **1983**, *24* (4), 469–472.
- (28) Baliga, S.; Wong, W. T. Depolymerization of Poly(ethylene terephthalate) Recycled from Post-Consumer Soft-Drink Bottles. *J. Polym. Sci., Part A: Polym. Chem.* **1989**, *27* (6), 2071–2082.
- (29) Kurokawa, H.; Ohshima, M.-A.; Sugiyama, K.; Miura, H. Methanolysis of Polyethylene Terephthalate (PET) in The Presence of Aluminium Triisopropoxide Catalyst to Form Dimethyl Terephthalate and Ethylene Glycol. *Polym. Degrad. Stab.* **2003**, *79* (3), 529–533.
- (30) Kamber, N. E.; Tsujii, Y.; Keets, K.; Waymouth, R. M.; Pratt, R. C.; Nyce, G. W.; Hedrick, J. L. The Depolymerization of Poly(ethylene terephthalate) (PET) Using *N*-Heterocyclic Carbenes from Ionic Liquids. *J. Chem. Educ.* **2010**, *87* (5), 519–521.
- (31) Fukushima, K.; Coulembier, O.; Lecuyer, J. M.; Almegren, H. A.; Alabdulrahman, A. M.; Alsewaleem, F. D.; McNeil, M. A.; Dubois, P.; Waymouth, R. M.; Horn, H. W.; Rice, J. E.; Hedrick, J. L. Organocatalytic Depolymerization of Poly(ethylene terephthalate). *J. Polym. Sci., Part A: Polym. Chem.* **2011**, *49* (5), 1273–1281.
- (32) Quaranta, E.; Sgherza, D.; Tartaro, G. Depolymerization of Poly(bisphenol A carbonate) under Mild Conditions by Solvent-Free Alcoholysis Catalyzed by 1,8-Diazabicyclo[5.4.0]undec-7-ene as a Recyclable Organocatalyst: A Route to Chemical Recycling of Waste Polycarbonate. *Green Chem.* **2017**, *19* (22), 5422–5434.
- (33) Do, T.; Baral, E. R.; Kim, J. G. Chemical Recycling of Poly(bisphenol A carbonate): 1,5,7-Triazabicyclo[4.4.0]-dec-5-ene Catalyzed Alcoholysis for Highly Efficient Bisphenol A and Organic Carbonate Recovery. *Polymer* **2018**, *143* (9), 106–114.
- (34) Fukushima, K.; Jones, G. O.; Horn, H. W.; Rice, J. E.; Kato, T.; Hedrick, J. L. Formation of Bis-Benzimidazole and Bis-Benzoxazole through Organocatalytic Depolymerization of Poly(ethylene terephthalate) and its Mechanism. *Polym. Chem.* **2020**, *11* (30), 4904–4913.
- (35) Saito, K.; Jehanno, C.; Meabe, L.; Olmedo-Martínez, J. L.; Mecerreyes, D.; Fukushima, K.; Sardon, H. From Plastic Waste to Polymer Electrolytes for Batteries through Chemical Upcycling of Polycarbonate. *J. Mater. Chem. A* **2020**, *8* (28), 13921–13926.
- (36) Jehanno, C.; Demartean, J.; Mantione, D.; Arno, M.; Ruiperez, F.; Hedrick, J.; Dove, A.; Sardon, H. Synthesis of Functionalized Cyclic Carbonates through Commodity Polymer Upcycling. *ACS Macro Lett.* **2020**, *9* (4), 443–447.
- (37) Saito, K.; Eisenreich, F.; Turel, T.; Tomovic, Z. Closed-Loop Recycling of Poly(imine-carbonate) Derived from Plastic Waste and Bio-Based Resources. *Angew. Chem., Int. Ed.* **2022**, *61* (43), No. e202211806.
- (38) Tan, M. Y.; Goh, L.; Safanama, D.; Loh, W. W.; Ding, N.; Chien, S. W.; Goh, S. S.; Thitsartarn, W.; Lim, J. Y. C.; Fam, D. W. H. Upcycling Waste Poly(ethylene terephthalate) into Polymer Electrolytes. *J. Mater. Chem. A* **2022**, *10* (46), 24468–24474.

- (39) Peng, Y.; Yang, J.; Deng, C.; Deng, J.; Shen, L.; Fu, Y. Acetolysis of Waste Polyethylene Terephthalate for Upcycling and Life-Cycle Assessment Study. *Nat. Commun.* **2023**, *14*, No. 3249.
- (40) Wang, X.-Y.; Gao, Y.; Tang, Y. Sustainable Developments in Polyolefin Chemistry: Progress, Challenges, and Outlook. *Prog. Polym. Sci.* **2023**, *143*, No. 101713.
- (41) Zhao, Y.; Li, D.; Jiang, X. Chemical Upcycling of Polyolefins through C–H Functionalization. *Eur. J. Org. Chem.* **2023**, *26* (39), No. e202300664.
- (42) Gandini, A.; Silvestre, A. J. D.; Neto, C. P.; Sousa, A. F.; Gomes, M. The Furan Counterpart of Poly(ethylene terephthalate): An Alternative Material Based on Renewable Resources. *J. Polym. Sci. Part A, Polym. Chem.* **2009**, *47* (1), 295–298.
- (43) Chatti, S.; Schwarz, G.; Kricheldorf, H. R. Cyclic and Noncyclic Polycarbonates of Isosorbide (1,4:3,6-Dianhydro-D-Glucitol). *Macromolecules* **2006**, *39* (26), 9064–9070.
- (44) Chen, Y.; Chen, Y.; Liu, L.; Zhang, Y.; Yuan, J. Microbial Synthesis of 4-Hydroxybenzoic Acid from Renewable Feedstocks. *Food Chem.: Mol. Sci.* **2021**, *3* (30), No. 100059.
- (45) Lin, C.-Y.; Tian, Y.; Nelson-Vasilchik, K.; Hague, J.; Kakumar, R.; Lee, M. Y.; Pidatala, V. R.; Trinh, J.; Ben, C. M. D.; Dalton, J.; Northen, T. R.; Baidoo, E. E. K.; Simmons, B. A.; Gladden, J. M.; Scown, C. D.; Putnam, D. H.; Kausch, A. P.; Sceller, H. V.; Eudes, A. Engineering Sorghum for Higher 4-Hydroxybenzoic Acid Content. *Metab. Eng. Commun.* **2022**, *15*, No. e00207.
- (46) Guo, X.; Wang, X.; Chen, T.; Lu, Y.; Zhang, H. Comparing *E. coli* Mono-Cultures and Co-Cultures for Biosynthesis of Protocatechuic Acid and Hydroquinone. *Biochem. Eng. J.* **2020**, *156*, No. 107518.
- (47) Zhao, M.; Hong, X.; Abdullah, Y.; Yao, R.; Xiao, Y. Rapid Biosynthesis of Phenolic Glycosides and their Derivatives from Biomass-Derived Hydroxycinnamates. *Green Chem.* **2021**, *23* (2), 838–847.
- (48) Jin, X.; Chung, T.-S. Thermal Decomposition Behavior of Main-Chain Thermotropic Liquid Crystalline Polymers, Vectra A-950, B-950, and Xyder SRT-900. *J. Appl. Polym. Sci.* **1999**, *73* (11), 2195–2207.
- (49) Lian, Z.; Bhawal, B. N.; Yu, P.; Morandi, B. Palladium-Catalyzed Carbon-Sulfur or Carbon-Phosphorus Bond Metathesis by Reversible Arylation. *Science* **2017**, *356* (6342), 1059–1063.
- (50) Tian, Z.; Shao, X.; Zhang, J.; Su, L.; Wang, Y.; Deng, T.; Wang, Y.; Hou, X. Chemical Recycling of Waste Poly-*p*-Phenylene Terephthamide via Selective Cleavage of Amide Bonds Catalyzed by Strong Brønsted Base in Alcohols. *Waste Manage.* **2022**, *137*, 275–282.
- (51) Minami, Y.; Matsuyama, N.; Takeichi, Y.; Watanabe, R.; Mathew, S.; Nakajima, Y. Depolymerization of Robust Polyetheretherketone to Regenerate Monomer Units Using Sulfur Reagents. *Commun. Chem.* **2023**, *6* (1), No. 14.
- (52) Minami, Y.; Inagaki, Y.; Tsuyuki, T.; Sato, K.; Nakajima, Y. Hydroxylation-Depolymerization of Oxyphenylene-Based Super Engineering Plastics to Regenerate Arenols. *JACS Au* **2023**, *3* (8), 2323–2332.
- (53) Minami, Y.; Honobe, R.; Inagaki, Y.; Sato, K.; Yoshida, M. Alcoholysis of Oxyphenylene-Based Super Engineering Plastics Mediated by Readily Available Bases. *Polym. J.* **2024**, *56*, 369–377.
- (54) Pham, D. D.; Cho, J. Low-Energy Catalytic Methanolysis of Poly(ethyleneterephthalate). *Green Chem.* **2021**, *23* (1), 511–525.
- (55) Le, N. H.; Ngoc Van, T. T.; Shong, B.; Cho, J. Low-Temperature Glycolysis of Polyethylene Terephthalate. *ACS Sustainable Chem. Eng.* **2022**, *10* (51), 17261–17273.
- (56) Olazabal, I.; Luna, E.; De Meester, S.; Jehanno, C.; Sardon, H. Upcycling of BPA-PC into Trimethylene Carbonate by Solvent Assisted Organocatalysed Depolymerisation. *Polym. Chem.* **2023**, *14* (19), 2299–2307.
- (57) Fukushima, K.; Watanabe, Y.; Ueda, T.; Nakai, S.; Kato, T. Organocatalytic Depolymerization of Poly(trimethylene carbonate). *J. Polym. Sci.* **2022**, *60* (24), 3489–3500.
- (58) Watanabe, Y.; Kato, R.; Fukushima, K.; Kato, T. Degradable and Nanosegregated Elastomers with Multiblock Sequences of Biobased Aromatic Mesogens and Biofunctional Aliphatic Oligocarbonates. *Macromolecules* **2022**, *55* (23), 10285–10293.
- (59) Gautam, P.; Neha; Upadhyay, S. N.; Dubey, S. K. Bio-Methanol as a Renewable Fuel from Waste Biomass: Current Trends and Future Perspective. *Fuel* **2020**, *273*, No. 117783.
- (60) Parkhey, P. Biomethanol: Possibilities towards a Bio-Based Economy. *Biomass Convers. Biorefin.* **2022**, *12* (5), 1877–1887.
- (61) Javed, S.; Fisse, J.; Vogt, D. Optimization and Kinetic Evaluation for Glycolytic Depolymerization of Post-Consumer PET Waste with Sodium Methoxide. *Polymers* **2023**, *15* (3), 687.
- (62) Gazeau-Bureau, S.; Delcroix, D.; Martin-Vaca, B.; Bourissou, D.; Navarro, C.; Magnet, S. Organo-Catalyzed ROP of ϵ -Caprolactone: Methanesulfonic Acid Competes with Trifluoromethanesulfonic Acid. *Macromolecules* **2008**, *41* (11), 3782–3784.
- (63) Fukushima, K.; Coady, D. J.; Jones, G. O.; Almegren, H. A.; Alabdulrahman, A. M.; Alsewilem, F. D.; Horn, H. W.; Rice, J. E.; Hedrick, J. L. Unexpected Efficiency of Cyclic Amidine Catalysts in Depolymerizing Poly(ethylene terephthalate). *J. Polym. Sci., Part A: Polym. Chem.* **2013**, *51* (7), 1606–1611.
- (64) Quaranta, E.; Minischetti, C. C.; Tartaro, G. Chemical Recycling of Poly(bisphenol A carbonate) by Glycolysis under 1,8-Diazabicyclo[5.4.0]undec-7-ene Catalysis. *ACS Omega* **2018**, *3* (7), 7261–7268.
- (65) Zhang, L.; Nederberg, F.; Messman, J. M.; Pratt, R. C.; Hedrick, J. L.; Wade, C. G. Organocatalytic Stereoselective Ring-Opening Polymerization of Lactide with Dimeric Phosphazene Bases. *J. Am. Chem. Soc.* **2007**, *129* (42), 12610–12611.
- (66) Fan, C.; Zhang, L.; Zhu, C.; Cao, J.; Xu, Y.; Sun, P.; Zeng, G.; Jiang, W.; Zhang, Q. Efficient Glycolysis of PET Catalyzed by a Metal-Free Phosphazene Base: The Important Role of EG⁻. *Green Chem.* **2022**, *24* (3), 1294–1301.
- (67) Jehanno, C.; Pérez-Madrigal, M. M.; Demarteau, J.; Sardon, H.; Dove, A. P. Organocatalysis for Depolymerization. *Polym. Chem.* **2019**, *10* (2), 172–186.
- (68) Kamber, N. E.; Jeong, W.; Waymouth, R. M.; Pratt, R. C.; Lohmeijer, B. G. G.; Hedrick, J. L. Organocatalytic Ring-Opening Polymerization. *Chem. Rev.* **2007**, *107* (12), 5813–5840.
- (69) Tshepelevitsh, S.; Kütt, A.; Lökov, M.; Kaljurand, I.; Saame, J.; Heering, A.; Pliieger, P. G.; Vianello, R.; Leito, I. On the Basicity of Organic Bases in Different Media. *Eur. J. Org. Chem.* **2019**, *2019* (40), 6735–6748.
- (70) Vazdar, K.; Margetic, D.; Kovacevic, B.; Sundermeyer, J.; Leito, I.; Jahn, U. Design of Novel Uncharged Organic Superbases: Merging Basicity and Functionality. *Acc. Chem. Res.* **2021**, *54* (15), 3108–3123.
- (71) Pratt, R. C.; Lohmeijer, B. G. G.; Long, D. A.; Waymouth, R. M.; Hedrick, J. L. Triazabicyclodecene: A Simple Bifunctional Organocatalyst for Acyl Transfer and Ring-Opening Polymerization of Cyclic Esters. *J. Am. Chem. Soc.* **2006**, *128* (14), 4556–4557.
- (72) Kaiho, S.; Hmayed, A. A. R.; Delle Chiaie, K. R.; Worch, J. C.; Dove, A. P. Designing Thermally Stable Organocatalysts for Poly(ethylene terephthalate) Synthesis: Toward a One-Pot, Closed-Loop Chemical Recycling System for PET. *Macromolecules* **2022**, *55* (23), 10628–10639.
- (73) Jehanno, C.; Flores, I.; Dove, A. P.; Müller, A. J.; Ruipérez, F.; Sardon, H. Organocatalysed Depolymerisation of PET in a Fully Sustainable Cycle Using Thermally Stable Protic Ionic Salt. *Green Chem.* **2018**, *20* (6), 1205–1212.
- (74) Wang, L.; Nelson, G. A.; Toland, J.; Holbrey, J. D. Glycolysis of PET Using 1,3-Dimethylimidazolium-2-Carboxylate as an Organocatalyst. *ACS Sustainable Chem. Eng.* **2020**, *8* (35), 13362–13368.
- (75) Luna, E.; Olzabal, I.; Roosen, M.; Müller, A.; Jehanno, C.; Ximenis, M.; Meester, S. D.; Sardon, H. Towards a Better Understanding of the Cosolvent Effect on the Low-Temperature Glycolysis of Polyethylene Terephthalate (PET). *Chem. Eng. J.* **2024**, *482*, No. 148861.

(76) Prasad, V. S.; Pillai, C. K. S. Copolyesters of Hydroxyphenylalkanoic Acids: Synthesis, Properties, and *In Vitro* Degradation of Poly(4-oxybenzoate-co-4-oxyphenylacetate). *J. Polym. Sci., Part A: Polym. Chem.* **2001**, *39* (5), 693–705.

(77) Prasad, V. S.; Pillai, C. K. S.; Krichendorf, H. R. Biodegradable Liquid Crystalline Polyesters of Hydroxyphenylalkanoic Acids: Synthesis and *In Vitro* Degradation Studies of Poly[3-(4-oxyphenyl)-propionate-co-4-oxybenzoate]. *J. Macromol. Sci., Part A: Pure Appl. Chem.* **2001**, *38* (7), 641–657.

(78) Leibfarth, F. A.; Moreno, N.; Hawker, A. P.; Shand, J. D. Transforming Polylactide into Value-Added Materials. *J. Polym. Sci., Part A: Polym. Chem.* **2012**, *50* (23), 4814–4822.

(79) Sawyer, L. C.; Jaffe, M. The Structure of Thermotropic Copolyesters. *J. Mater. Sci.* **1986**, *21*, 1897–1913.

(80) Dreher, S.; Seifert, S.; Zachmann, H. G.; Moszner, N.; Mercoli, P.; Zanghellini, G. Chain Orientation in Melt-Extruded Samples of Vectra A, Vectra B, and Blends in Relation to The Mechanical Properties. *J. Appl. Polym. Sci.* **1998**, *67*, 531–545.

(81) Kaito, A.; Kyotani, M.; Nakayama, K. Effects of Annealing on the Structure Formation in a Thermotropic Liquid Crystalline Copolyester. *Macromolecules* **1990**, *23* (4), 1035–1040.

(82) Wilson, D. J.; Vonk, C. G.; Windle, A. H. Diffraction Measurements of Crystalline Morphology in a Thermotropic Random Copolymer. *Polymer* **1993**, *34* (2), 227–237.

(83) Romo-Uribe, A.; Reyes-Mayer, A.; Rodriguez, M. C.; Sarmiento-Bustos, E. On The Influence of Thermal Annealing on Molecular Relaxations and Structure in Thermotropic Liquid Crystalline Polymer. *Polymer* **2022**, *240*, No. 124506.

(84) Sun, Z.; Cheng, H.-M.; Blackwell, J. Structure of Annealed Copoly(*p*-hydroxybenzoic acid-2-hydroxy-6-naphthoic acid). 1. Chain Conformation and Packing. *Macromolecules* **1991**, *24* (14), 4162–4167.

(85) Windle, A. H.; Viney, C.; Golombok, R.; Donald, A. M.; Mitchel, G. R. Molecular Correlation in Thermotropic Copolyesters. *Faraday Discuss. Chem. Soc.* **1985**, *79*, 55–72.

(86) Sarlin, J.; Tormala, P. Isothermal Heat Treatment of a Thermotropic LCP Fiber. *J. Polym. Sci., Part B: Polym. Phys.* **1991**, *29* (4), 395–405.

(87) Chang-Chien, G.-P.; Denn, M. M. Isothermal Crystallization Kinetics of Poly(ethylene terephthalate) in Blends with a Liquid Crystalline Polyester (Vectra A). *Polym. Adv. Technol.* **1996**, *7* (3), 168–172.

(88) Iwasaki, T.; Tsuge, K.; Naito, N.; Nozaki, K. Chemoselectivity Change in Catalytic Hydrogenolysis Enabling Urea-Reduction to Formamide/Amine Over More Reactive Carbonyl Compounds. *Nat. Commun.* **2023**, *14*, No. 3279.

(89) Akerlof, G. Dielectric Constants of Some Organic Solvent-Water Mixtures at Various Temperatures. *J. Am. Chem. Soc.* **1932**, *54* (11), 4125–4139.